Draft version August 13, 2021
Typeset using LaTeX **preprint2** style in AASTeX631

Calculations of the Black Hole Masses in IC 2560 and UGC 3193

Alina Kaliszewski[1,2] and Jim Braatz[2]

[1] *University of Minnesota Department of Physics and Astronomy*
116 Church St SE
Minneapolis, MN 55455, USA
[2] *National Radio Astronomy Observatory*
520 Edgemont Road
Charlottesville, VA 22903, USA

ABSTRACT

Using circumnuclear water maser observations obtained from the Green Bank Telescope (GBT) and the Very Long Baseline Array (VLBA), we calculated the masses of the supermassive black holes (SMBHs) at the center of the active galactic nucleus (AGN) galaxies IC 2560 and UGC 3193. The SMBH mass for IC 2560, as measured by maser emission in Keplerian rotation around the black hole, was found to be $(5.3 \pm 0.2) \times 10^6\ M_\odot$. We determined the upper limit on the SMBH mass for UGC 3193 to be $(0.6 \pm 0.02) \times 10^6 M_\odot$. The maser emission for UGC 3193 is likely occurring outside of the SMBH's gravitational sphere of influence, so our calculations reflect the enclosed mass. A preliminary geometric distance to IC 2560 was also calculated to be $39.3^{+1.2}_{-0.9}$ Mpc, which is consistent with other distances calculated using the 21cm velocity of 2923 ± 10 km s^{-1} and the most recent value of the Hubble constant published by the Megamaser Cosmology Project, 73.9 ± 3.0 km s^{-1} Mpc^{-1}.

1. INTRODUCTION

By observing water maser emission in active galactic nucleus galaxies (AGNs), it is possible to determine the masses of the supermassive black holes (SMBHs) at the centers of these galaxies, the distances to the galaxies, and orientation parameters associated with the maser disk. Water maser emission occurs at a frequency of 22 GHz, and can be observed with the Green Bank Telescope (GBT) and the Very Long Baseline Array (VLBA). Masers are dynamical tracers, which allow for very precise measurements of their positions and velocities.

Edge-on maser disks display triple peaked maser emission patterns. Triple peaked masers typically exhibit emission at the galaxy's systemic velocity, in addition to symmetrical red- and blueshifted features centered around the systemic features. The systemic features arise on the near side of the edge-on disk. The red- and blueshifted features arise on the tangential edges of the disk, rotating away from (redshifted) or toward (blueshifted) the observer. The positions and velocities of maser features, obtained through Very Long Baseline Interferometry (VLBI), can be used to determine the mass of the central black hole. When combined with these positions and velocities, the measured centripetal accelerations of individual maser components allow for determination of the distance to the galaxy.

Megamasers, emitted by Seyfert 2 or LINER active galactic nucleus galaxies (AGNs), display isotropic luminosities of approximately 6

orders of magnitude higher than average Galactic masers (Braatz & Gugliucci 2008). Circumnuclear H_2O megamasers typically form in disks less than 1 pc from their central black holes (Lo 2005). The megamaser disks which we can detect are edge-on to our line of sight, and the centripetal acceleration typically exhibits Keplerian rotation. Maser disks may occur at many different orientations, but an inclination angle away from our line of sight results in a shorter gain path and hence a smaller amplification factor. A maser disk which does not display Keplerian rotation is often an indication that there are additional gravitational forces acting on the disk.

SMBH masses in maser systems are typically on the scale of $10^6 M_\odot$ to $10^7 M_\odot$ (Pesce et al. 2020b; Braatz et al. 2010; Gao et al. 2017). Other black hole mass measurement techniques include the use of gravitational waves or mapping reverberations of AGN continuum emission (Yu & Chen 2021). The $M_{BH}-\sigma$ relation places typical black hole masses in the range of $10^5 M_\odot$ to $10^{10} M_\odot$ (Bennert et al. 2015; Zhou et al. 2021). Optical telescopes can be used to determine BH masses in elliptical galaxies (e.g. Rey et al. (2021)), but dusty nuclei in spiral galaxies obscure less massive black holes. Radio emission is unaffected by this dust, so masers can be used to study these less massive black holes (Blain et al. 2004).

The Megamaser Cosmology Project is using masers to investigate the Hubble tension, as geometric distances to masers provide an independent alternative to the distance ladder constructed using Cepheid Variables. The maser technique requires high precision VLBI maps and acceleration data, and their methods are described in Reid et al. (2009).

Maser emission was first detected in IC 2560 in 1994 (Braatz et al. 1994) and in UGC 3193 in 2008 (Braatz & Gugliucci 2008). There is no maser emission observed at the systemic velocity of UGC 3193, despite symmetric red- and blueshifted emission (Braatz & Gugliucci 2008). IC 2560 does exhibit observable maser emission at its systemic velocity, which makes it a candidate for calculating its distance using masers, due to the nonzero accelerations of the systemic components. Jan Wagner (private communication) used VLBI imaging and GBT data to study the kinematics of both UGC 3193 and IC 2560 with a model fitting technique predating the MCP's current 3 dimensional Monte Carlo Markov Chain (MCMC) approach.

2. IMPROVED BLACK HOLE MASS ESTIMATES

Previous studies of maser emission have involved model fitting techniques such as those described in Reid et al. (2009), Braatz et al. (2010), and Yamauchi et al. (2012). We analyzed the kinematic data obtained from Wagner's observations using a 3 dimensional MCMC model written in Python by Dom Pesce (Pesce et al. 2020b). Pesce's 3 dimensional model received inputs such as the positions of the maser emission, obtained using VLBI data, the velocities of each maser point, obtained using spectral analysis, and line-of-sight accelerations for each maser component. We determined individual maser component accelerations by visually identifying peaks in galaxy emission spectra from approximately monthly GBT monitoring observations and fitting a straight line through the peaks from multiple epochs (see Figure 1).

The model fitted a 3 dimensional disk with warping considered in the directions of both the position and inclination angles (see Appendix B for an input control file). It output the results of the MCMC fitting as median values with confidence intervals for global parameters such as the black hole mass, position, and recession velocity, in addition to the distance to the galaxy and maser disk warping parameters (Pesce et al. 2020b).

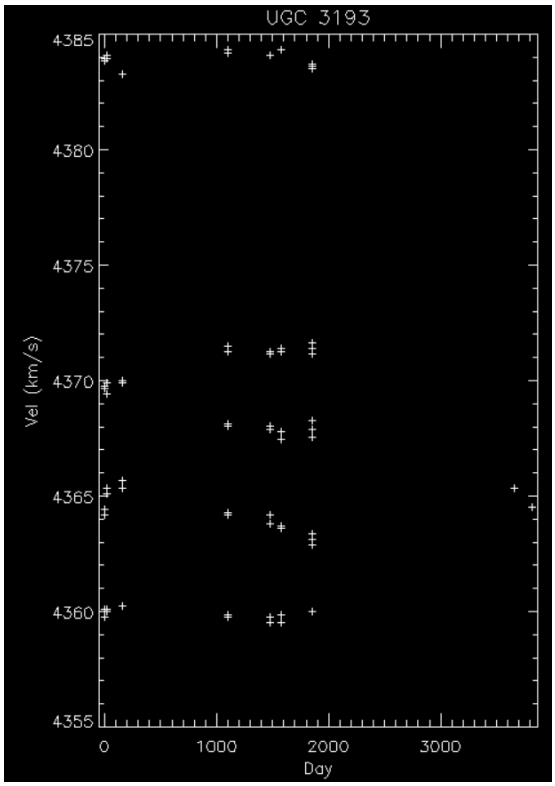

Figure 1. Velocity vs Time Plot for Acceleration Calculations

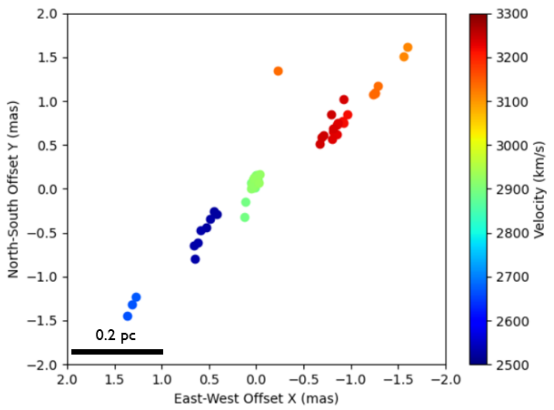

Figure 2. VLBI Map for IC 2560

2.1. *IC 2560*

The VLBI map for IC 2560 (see Figure 2) was constructed using only data points with SNR values greater than 5 (see Appendix A). The orange data point at (-0.226, 1.345) was assigned to be the result of black hole outflow or other gas and dust unrelated to the maser disk. As a result, this point was not included in the disk model fitting. This map shows that the maser disk has a diameter of just below 1 pc, which is typical for edge-on maser disks.

We separated IC 2560's maser features into 4 different groups for model fitting in order to study the maser disk's behavior at different radii. The inner features, which do not include the systemic components, were located at radii less than 0.3 pc, and the outer features were located at radii greater than 0.3 pc. We also studied trials involving both the inner and outer components, and all maser emission (i.e., inner and outer plus systemic). These 4 trials are displayed in Table 1. All trials were fit with a flat maser disk, due to the lack of visible warping in IC 2560's VLBI map.

For the first 3 trials, the distance to the galaxy was set to a fixed value of 39.6 ± 1.6 Mpc. This distance was calculated using the 21cm line velocity of 2923 ± 10 km s^{-1} and the Hubble constant value of 73.9 ± 3.0 km s^{-1} Mpc^{-1} published by the Megamaser Cosmology Project in 2020 (Pesce et al. 2020a). When the accelerations from the systemic maser features were included in the final trial, the model fitted the geometric distance to the galaxy using a uniform prior. For all trials, the model fitted both the SMBH mass and the maser disk's position angle using a uniform prior.

2.2. *UGC 3193*

The VLBI map for UGC 3193 (see Figure 3) shows a maser disk diameter of 2-3 pc, which is more extended than typically expected for a maser of this type. Previous measurements of similar maser disks have resulted in sub-pc diameters ranging from 0.18 pc to 0.6 pc (Braatz & Gugliucci 2008; Braatz et al. 2010). Because UGC 3193 displays no detectable maser emission at its systemic velocity, we were unable to fit the distance to the galaxy. In order to determine a SMBH mass, we adopted a fixed distance of 60.3 ± 2.5 Mpc, calculated using the HI line velocity of 4454 ± 10 km s^{-1} and the Megamaser

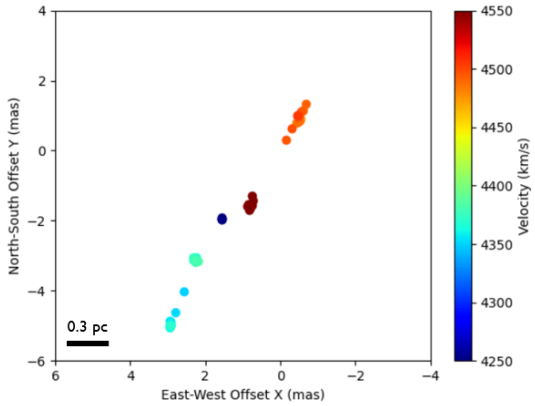

Figure 3. VLBI Map for UGC 3193

Cosmology Project's Hubble constant value of 73.9 ± 3.0 km s^{-1} Mpc^{-1} (Pesce et al. 2020a). The radial structure of the maser shows a pronounced kink, which we attempted to fit using second order warping parameters. To explore the behavior of maser components at different radii, we ran several trials of the model fit. For some iterations, we limited the data to only the inner or outer maser features. We defined the inner maser components to be those at a radius less than 0.3 pc and the outer maser components to be those at a radius greater than 0.3 pc. The trials for each individual ring were run with the assumption of a flat maser disk. We also conducted a trial using both the inner and outer (i.e., all data points, see Appendix A) features. This trial made use of the model's 3D warp fitting capabilities to take into account the visible warp in the middle of the VLBI map. The SMBH mass and position angle of the maser disk were both calculated using uniform priors. These results are shown in Table 2.

3. RESULTS AND DISCUSSION

3.1. *IC 2560*

The SMBH mass values from different trial runs are within 1-2σ of each other, with the exception of the trial using only the outer maser components. There were only 9 maser components designated as outer features at a radius greater than 0.3 pc, and the uncertainties are higher in this trial than in others. The outlier points at (-0.226, 1.345) were omitted. The trial run on the outer maser components resulted in a mass of $(4.6^{+0.4}_{-0.3}) \times 10^6 M_\odot$, while the other trials ranged from $(5.3 \pm 0.2) \times 10^6 M_\odot$ to $(5.6 \pm 0.2) \times 10^6 M_\odot$. These masses are all in the lower end of the range of typical maser system SMBH masses. The geometric distance calculated by the model fit for IC 2560, $39.3^{+1.2}_{-0.9}$ Mpc, is within 1σ of the value of 39.6 ± 1.6 Mpc calculated using the 21cm velocity and H_0.

The position angle values range from $-45.9^{+1.2}_{-1.1}$ degrees to $-49.2^{+0.7}_{-0.7}$ degrees. The lower bound of this range is in agreement with Yamauchi et al. (2012), and the range is consistent with visual observations of the VLBI map.

3.2. *UGC 3193*

The central masses for UGC 3193 are not in agreement with each other, ranging from $(0.6 \pm 0.2) \times 10^6 M_\odot$ to $(1.2 \pm 0.03) \times 10^6 M_\odot$. The smallest value, which comes from the trial using only the inner maser components, is below the range of typical maser galaxy SMBH masses, but the trials run using the outer and all maser components result in mass values within the low end of the typical range for maser systems. Taking into consideration the large maser disk diameter and relatively low rotation velocities and mass values, it is likely that the maser emission is occurring outside of the gravitational sphere of influence of the black hole. This would indicate that we are seeing the enclosed mass as opposed to the black hole mass. This idea is also supported by the fact that the enclosed mass value increases as the radius of the fitted features increases.

The wide range of position angles, from -30.2 ± 0.2 degrees to -68.8 ± 2.0 degrees, is

Table 1. IC 2560

Inner or Outer	Distance Prior	Distance (Mpc)	Mass ($10^7 M_\odot$)	Ω_0 (degrees)
I	F	$39.6^{+1.6}_{-1.6}$	$0.56^{+0.02}_{-0.02}$	$-48.6^{+1.3}_{-1.4}$
O	F	$39.6^{+1.6}_{-1.6}$	$0.46^{+0.04}_{-0.03}$	$-45.9^{+1.2}_{-1.1}$
I+O	F	$39.6^{+1.6}_{-1.6}$	$0.56^{+0.02}_{-0.01}$	$-47.5^{+0.8}_{-0.9}$
All	U	$39.3^{+1.2}_{-0.9}$	$0.53^{+0.02}_{-0.02}$	$-49.2^{+0.7}_{-0.7}$

NOTE—Column 1 indicates which maser features were analyzed. Column 2 indicates whether the distance was set to a fixed value or fit to a uniform prior. Column 5 contains the position angle of the maser disk.

Table 2. UGC 3193

Inner or Outer	Distance Prior	Distance (Mpc)	Mass ($10^7 M_\odot$)	Ω_0 (degrees)
I	F	$60.3^{+2.5}_{-2.5}$	$0.06^{+0.02}_{-0.02}$	$-63.8^{+2.0}_{-2.0}$
O	F	$60.3^{+2.5}_{-2.5}$	$0.10^{+0.01}_{-0.01}$	$-30.2^{+0.2}_{-0.2}$
All	F	$60.3^{+2.5}_{-2.5}$	$0.12^{+0.003}_{-0.003}$	$-68.8^{+3.6}_{-3.7}$

NOTE—Column 1 indicates which maser features were analyzed. Column 2 indicates whether the distance was set to a fixed value or fit to a uniform prior. Column 5 contains the position angle of the maser disk.

due to the shape of the maser disk seen in UGC 3193's VLBI map. The warp visible in the inner maser features results in a much larger position angle than is seen when analyzing the outer data points. It is likely that the lack of observed systemic maser emission is a result of the disk warp or the maser disk being offset by some angle from our line of sight.

4. CONCLUSION

Using a 3 dimensional Monte Carlo Markov Chain model fit on maser emission data, we calculated the mass of the supermassive black hole at the center of the Seyfert 2 galaxy IC 2560 to be $(5.3 \pm 0.2) \times 10^6 M_\odot$. Following a similar method, we also calculated the enclosed mass in the region around the supermassive black hole at the center of UGC 3193 to have an upper limit of $(0.6 \pm 0.02) \times 10^6 M_\odot$. Preliminary calculations also resulted in a geometric distance to IC 2560 of $39.3^{+1.2}_{-0.9}$ Mpc, which supports the current value of H_0 from the Megamaser Cosmology Project. Further analysis of this galaxy is necessary to confirm this value.

The National Radio Astronomy Observatory is a facility of the National Science Foundation operated under cooperative agreement by Associated Universities, Inc. This research has made use of the NASA/IPAC Extragalactic Database (NED), which is operated by the Jet Propulsion Laboratory, California Institute of Tech-

nology, under contract with the National Aeronautics and Space Administration This research was conducted as part of the National Radio Astronomy Observatory's Research Experience for Undergraduates (REU) program, funded by the National Science Foundation.

Facilities: GBT, VLBA

Software: GBTIDL, PyMC3

APPENDIX

A. MASER DATA

Table 3. Data for IC 2560

Velocity (km/s)	X (mas)	Error in X	Y (mas)	Error in Y	SNR
2522.99	0.416	0.050	-0.292	0.122	5.3
2523.84	0.526	0.064	-0.437	0.178	5.3
2524.70	0.452	0.038	-0.257	0.114	7.1
2525.56	0.485	0.037	-0.345	0.108	6.4
2528.13	0.585	0.039	-0.469	0.098	7.0
2528.98	0.615	0.030	-0.611	0.086	7.8
2529.84	0.651	0.044	-0.795	0.132	5.5
2530.70	0.660	0.051	-0.642	0.133	5.4
2665.40	1.365	0.061	-1.447	0.153	5.4
2666.26	1.312	0.033	-1.314	0.095	8.9
2671.41	1.277	0.058	-1.228	0.177	5.2
2890.26	0.017	0.033	0.042	0.088	6.9
2891.12	-0.020	0.040	0.104	0.121	6.3
2891.98	0.012	0.029	0.020	0.091	7.9
2892.84	0.127	0.030	-0.324	0.108	7.4
2893.70	0.115	0.025	-0.147	0.071	9.0
2894.56	0.051	0.018	0.071	0.055	10.7
2895.42	0.029	0.016	0.123	0.048	12.8
2986.28	0.027	0.015	0.073	0.041	15.6
2897.14	0.036	0.013	0.054	0.036	17.9
2897.99	0.034	0.013	0.063	0.035	18.3
2898.85	0.027	0.014	0.107	0.038	17.1
2899.71	0.045	0.012	0.063	0.035	18.2
2900.57	0.038	0.011	0.050	0.030	21.1
2901.43	0.032	0.010	0.064	0.028	23.7
2902.29	0.032	0.008	0.071	0.023	28.0
2903.15	0.027	0.009	0.106	0.024	26.2
2904.01	0.028	0.009	0.125	0.025	25.1
2904.87	0.039	0.009	0.084	0.025	25.2
2905.73	0.029	0.011	0.103	0.030	21.7

Velocity (km/s)	X (mas)	Error in X	Y (mas)	Error in Y	SNR
2906.58	0.025	0.010	0.110	0.026	24.1
2907.44	0.002	0.010	0.155	0.028	22.2
2908.30	-0.002	0.011	0.156	0.031	20.2
2909.16	0.018	0.012	0.091	0.032	19.5
2910.02	0.029	0.012	0.088	0.032	19.5
2910.88	0.030	0.012	0.103	0.033	19.3
2911.74	0.024	0.013	0.116	0.035	16.8
2912.60	0.005	0.010	0.139	0.030	20.6
2913.46	0.009	0.009	0.107	0.026	24.4
2914.32	0.017	0.012	0.099	0.031	21.1
2915.18	0.016	0.013	0.125	0.034	18.4
2916.04	0.036	0.018	0.053	0.051	13.0
2916.89	0.033	0.020	0.020	0.057	12.6
2917.75	0.032	0.025	0.056	0.070	9.5
2918.61	0.058	0.022	0.007	0.062	9.3
2919.47	0.042	0.019	0.047	0.053	10.9
2920.33	0.029	0.023	0.082	0.057	11.1
2921.19	0.022	0.034	0.038	0.088	7.2
2922.05	0.027	0.035	0.127	0.111	5.2
2922.91	-0.036	0.036	0.163	0.095	5.3
2928.06	-0.022	0.028	0.064	0.073	5.9
3114.42	-1.563	0.054	1.510	0.137	5.8
3115.28	-1.599	0.046	1.621	0.124	6.0
3135.04	-0.226	0.054	1.345	0.126	5.2
3136.76	-1.288	0.053	1.175	0.179	5.8
3136.79	-1.259	0.021	1.092	0.058	15.1
3137.62	-1.237	0.047	1.074	0.142	6.5
3137.65	-1.255	0.023	1.091	0.063	13.7
3216.80	-0.914	0.076	0.771	0.181	5.0
3217.66	-0.964	0.032	0.844	0.090	9.0
3218.52	-0.921	0.040	0.750	0.113	7.0
3228.85	-0.848	0.053	0.734	0.161	5.5
3229.71	-0.809	0.029	0.653	0.087	9.1
3230.57	-0.856	0.044	0.625	0.112	7.7
3233.15	-0.867	0.047	0.754	0.143	6.2
3234.01	-0.802	0.054	0.564	0.186	5.5
3239.18	-0.923	0.058	1.025	0.173	6.1
3240.04	-0.813	0.058	0.686	0.170	5.7
3242.62	-0.668	0.056	0.518	0.143	5.8

Velocity (km/s)	X (mas)	Error in X	Y (mas)	Error in Y	SNR
3243.49	-0.695	0.042	0.594	0.109	8.6
3244.35	-0.707	0.039	0.613	0.091	7.7
3246.07	-0.795	0.054	0.847	0.164	5.8

NOTE—Model fitting trials were run on subsets of this data. The point at (-0.226, 1.345) was omitted during all trials. Data from Wagner (private communication).

Table 4. Data for UGC 3193

Velocity (km/s)	X (mas)	Error in X	Y (mas)	Error in Y	SNR
4241.56	1.575	0.009	-1.926	0.034	21.4
4243.29	1.564	0.006	-1.921	0.024	31.8
4245.02	1.577	0.007	-1.950	0.027	28.9
4246.76	1.564	0.009	-1.950	0.034	22.7
4349.08	2.570	0.072	-4.009	0.168	6.0
4350.81	2.789	0.026	-4.624	0.072	12.0
4352.55	2.913	0.007	-4.936	0.023	33.0
4354.28	2.936	0.004	-4.889	0.015	48.6
4356.02	2.950	0.003	-4.850	0.010	69.8
4357.75	2.946	0.002	-5.034	0.009	89.5
4359.49	2.943	0.002	-5.048	0.007	102.3
4361.22	2.947	0.002	-4.970	0.007	102.0
4362.96	2.945	0.002	-4.995	0.007	99.0
4364.69	2.937	0.002	-4.982	0.007	108.3
4366.43	2.243	0.021	-3.033	0.068	9.4
4366.43	2.931	0.002	-4.977	0.007	98.8
4368.16	2.272	0.016	-3.073	0.057	12.1
4368.16	2.926	0.003	-4.983	0.010	69.7
4369.90	2.920	0.007	-5.005	0.026	28.5
4369.90	2.320	0.013	-3.048	0.045	16.3
4371.63	2.320	0.013	-3.098	0.039	18.3
4373.37	2.329	0.012	-3.069	0.038	18.0
4375.10	2.308	0.014	-3.139	0.048	15.7
4376.84	2.282	0.012	-3.193	0.040	18.8
4378.57	2.273	0.006	-3.153	0.022	33.1
4380.31	2.258	0.008	-3.095	0.028	26.0
4382.04	2.206	0.032	-3.156	0.091	8.4
4476.67	-0.497	0.007	0.908	0.025	31.3
4478.41	-0.516	0.004	0.924	0.014	52.3
4480.14	-0.515	0.005	0.884	0.016	44.7
4481.88	-0.500	0.005	0.838	0.018	42.2
4483.62	-0.495	0.006	0.876	0.020	37.5
4485.35	-0.437	0.014	0.792	0.040	22.2
4487.09	-0.471	0.022	0.823	0.064	15.4
4488.83	-0.479	0.016	0.848	0.047	18.0
4490.56	-0.594	0.012	1.151	0.033	27.1
4492.30	-0.677	0.007	1.351	0.021	38.4
4494.04	-0.548	0.020	1.112	0.048	23.0
4495.77	-0.149	0.036	0.321	0.087	15.1
4497.51	-0.300	0.021	0.630	0.054	21.6

Velocity (km/s)	X (mas)	Error in X	Y (mas)	Error in Y	SNR
4499.24	-0.459	0.005	0.975	0.016	46.0
4500.98	-0.467	0.003	0.987	0.011	65.2
4502.72	-0.470	0.004	1.001	0.013	54.6
4504.45	-0.463	0.016	1.005	0.050	14.0
4564.07	0.751	0.045	-1.293	0.162	5.2
4565.80	0.727	0.017	-1.424	0.062	12.2
4565.80	0.799	0.013	-1.629	0.051	14.4
4569.28	0.866	0.018	-1.528	0.068	11.8
4571.01	0.839	0.018	-1.607	0.065	12.0
4572.75	0.837	0.017	-1.684	0.055	14.0
4574.49	0.876	0.023	-1.593	0.081	10.6
4576.23	0.806	0.021	-1.566	0.088	9.0
4577.96	0.773	0.024	-1.549	0.091	7.6
4579.70	0.763	0.032	-1.552	0.115	5.5

NOTE—Model fitting trials were run on subsets of this data. Data from Wagner (private communication).

B. SAMPLE CONTROL FILE

The control file designates lower and upper bounds for the model fitting parameters, as well as the prior applied when fitting each parameter. It also sets various MCMC parameters, beam parameters, and important velocities related to the maser emission.

```
%============================================================================%
%----------------Lower and upper bounds for every parameter-----------------%
%============================================================================%
% U = uniform prior
% N = normal (Gaussian) prior
% C = "combined" prior; only applicable for D and M (this prior makes an internal
%      transformation from D and M to M/D and M/D^2, which may speed up sampling)
% F = hold this parameter fixed (it will be held fixed at the "guess" value)
%
% Guess         Lower bound    Upper bound      Prior
%
 60.3           57.8           62.8             F          % Distance (in Mpc)
 1.0            0.01           10.0             U          % BH mass (in 10^7
                                                             solar masses)
 4400.0         4000.0         5000.0           U          % BH velocity (in
                                                             km/s); note: should
                                                             use the same frame
                                                             + convention as the
                                                             input maser
                                                             velocities
 1.2            0.0            3.0              U          % BH x-position (in
                                                             mas)
 -1.8          -3.0            0.0              U          % BH y-position (in
                                                             mas)
 90.0           70.0           110.0            U          % i_0 (inclination
                                                             angle in degrees,
                                                             with 90 being
                                                             edge-on)
 0.0           -100.0          100.0            F          % di/dr (in
                                                             degrees/mas)
 0.0           -100.0          100.0            F          % d^2i/dr^2 (in
                                                             degrees/mas/mas)
 -30.0         -180.0          180.0            U          % Omega_0 (position
                                                             angle in degrees)
 0.0           -100.0          100.0            F          % dOmega/dr (in
                                                             degrees/mas)
 0.0           -100.0          100.0            F          % d^2Omega/dr^2 (in
                                                             degrees/mas/mas)
```

```
 % Guess        Lower Bound    Upper Bound     Prior
 0.0            0.0            360.0             F          % omega_0 (periapsis
                                                             angle in degrees)
 0.0           -100.0          100.0             F          % domega/dr (in
                                                             degrees/mas)
 0.0           -100.0          100.0             F          % d^2omega/dr^2 (in
                                                             degrees/mas/mas)
 0.0            0.0            1.0               F          % orbital eccentricity
 1.00           0.1            10.0              F          % beam scaling
                                                             parameter for
                                                             position errors
                                                             (unitless)
 0.01           0.0            1.0               F          % x-position error
                                                             floor (in mas)
 0.01           0.0            1.0               F          % y-position error
                                                             floor (in mas)
 2.0            0.0            20.0              F          % velocity error floor
                                                             for high-velocity
                                                             features (in km/s)
 2.0            0.0            20.0              F          % velocity error floor
                                                             for systemic
                                                             features (in km/s)

 0.5            0.0            10.0              F          % acceleration error
                                                             floor (in km/s/yr)
%
 0.2            0.01           5.0               U          % redshifted feature
                                                             radii (in mas)
 90.0           45.0           135.0             U          % redshifted feature
                                                             azimuthal angle (in
                                                             degrees)
%
 0.2            0.01           10.0              U          % blueshifted feature
                                                             radii (in mas)
 -90.0         -135.0         -45.0              U          % blueshifted feature
                                                             azimuthal angle (in
                                                             degrees)
%
 2.0            0.01           10.0              U          % systemic feature
                                                             radii (in mas)
 0.0           -45.0           45.0              U          % systemic feature
                                                             azimuthal angle (in
                                                             degrees)
```

```
%
 0.0           -20.0            20.0             U          % acceleration value
                                                              for maser spots with
                                                              unmeasured
                                                              accelerations (in
                                                              km/s/yr)
%
%===============================================================================%
%-----------------MCMC parameters-----------------------------------------------%
%===============================================================================%
%
1000                    % Number of burn-in trials to use
10000                   % Total number of MCMC trials to run after burn-in
1                       % Factor by which to "thin" the output parameter file
100                     % Factor by which to "thin" the output maser spot files
1                       % Number of simultaneous MCMC chains to run
HMC                     % Choice of sampler (HMC = Hamiltonian Monte Carlo,
                          MH = Metropolis-Hastings)
2223508                 % Set random seed for reproducibility (just use a random
                          integer)
0                       % Toggle for initial optimization; set to 1 to turn it on,
                          0 to turn it off
%
%===============================================================================%
%-----------------Various important velocities----------------------------------%
%===============================================================================%
%
% All velocities should be specified in km/s
%
4400              % Velocity delineating the blueshifted and systemic features
4470              % Velocity delineating the systemic and redshifted features
0.0               % Conversion between input data frame and CMB frame (such that
                    v_cmb = v_input + cmb_conversion)
%
%===============================================================================%
%-----------------Beam parameters for VLBI map----------------------------------%
%===============================================================================%
%
0.40                % Minor axis of the beam (in mas)
1.60                % Major axis of the beam (in mas)
-6.7                % Position angle of the beam (in degrees East of North)
0                   % Toggle for beam scaling; set to 1 to turn beam scaling on,
                      0 to turn it off
```

REFERENCES

Bennert, V. N., Treu, T., Auger, M. W., et al. 2015, ApJ, 809, 14, doi: 10.1088/0004-637X/809/1/20

Blain, A. W., Carilli, C., & Darling, J. 2004, 48, 1247, doi: 10.1016/j.newar.2004.09.009

Braatz, J. A., & Gugliucci, N. E. 2008, ApJ, 678, 96, doi: 10.1086/529538

Braatz, J. A., Reid, M. J., Humphreys, E. M. L., et al. 2010, ApJ, 718, 657, doi: 10.1088/0004-637X/718/2/657

Braatz, J. A., Wilson, A. S., & Henkel, C. 1994, AAS Meeting Abstracts, 26, 1342

Gao, F., Braatz, J. A., Reid, M. J., et al. 2017, ApJ, 834, 19, doi: 10.3847/1538-4357/834/1/52

Lo, K. Y. 2005, 43, 625, doi: 10.1146/annurev.astro.41.011802.094927

Pesce, D., Braatz, J., Reid, M., et al. 2020a, doi: 10.5281/zenodo.4062113

Pesce, D. W., Braatz, J. A., Reid, M. J., et al. 2020b, ApJ, 890, 15, doi: 10.3847/1538-4357/ab6bcd

Reid, M. J., Braatz, J. A., Condon, J. J., et al. 2009, ApJ, 695, 287, doi: 10.1088/0004-637X/695/1/287

Rey, S.-C., Oh, K., & Kim, S. 2021, 8, doi: 2107.10289

Yamauchi, A., Nakai, N., Ishihara, Y., Diamond, P., & Sato, N. 2012, PASJ, 64, 17, doi: 10.1093/pasj/64.5.103

Yu, H., & Chen, Y. 2021, 126, 5, doi: 10.1103/PhysRevLett.126.021101

Zhou, Z. Q., Liu, F. K., Komossa, S., et al. 2021, ApJ, 907, 26, doi: 10.3847/1538-4357/abcccb